

METHODOLOGICAL NOTES PACS numbers: **91.30. – f**, 91.45.Hc, 91.50.Wy

On some correlations in seismodynamics and on two components of Earth's seismic activity

A M Fridman, E V Polyachenko, N R Nasyrkanov

DOI: 10.3367/UFNe.0180.201003f.0303

Contents

1. **Introduction** **291**
2. **Two components of Earth's seismic activity** **293**
3. **M- and T-components in the most seismically active region of Earth** **294**
4. **The M-component of mid-oceanic ridges** **296**
5. **Analysis of seismicity of the Alps–Himalayas belt** **296**
6. **Earth's seismic activity as a function of latitude and its dependence on the depth of epicenters** **296**
7. **On the link between seismic activity and Earth's diurnal rotation** **297**
8. **Conclusions** **299**
9. **Appendix** **299**
References **299**

Abstract. **A brief critical review of papers published in *Fizika Zemli* is presented.**

"Seismology evolved later than the majority of the physical sciences. It is now just as difficult to imagine seismologists without their main instrument — the seismograph — as to imagine astronomers without telescopes. However, the telescope was built around 1600, while the first effective seismographs were made between 1879 and 1890."

C Richter. *Elementary Seismology* [1]

1. Introduction

Forecasting earthquakes requires the formulation of sufficient attributes for their occurrence, which are still unknown. In doing so, the main difficulty of seismological problems, as compared, for instance, to astronomical ones, is rooted not only in the fact that experimental seismology emerged much later than observational astronomy, but also in the complexity of Earth's interior structure, which makes the development of seismic dynamics exceptionally difficult. Namely for this reason, we find appealing first and foremost designing a phenomenological model for seismic activity (in much the same way as thermodynamics was formulated well in advance of statistical physics). This task requires, in particular, the knowledge of the correlations presented further in this paper. However, before embarking on a description of these fairly important correlations characterizing Earth's seismic activity $N(t)$, it should perhaps be explained, at least very briefly, how the quantity $N(t)$ is defined, e.g., how earthquakes are detected and their main characteristics are determined.

A M Fridman, E V Polyachenko Institute of Astronomy, Russian Academy of Sciences,
ul. Pyatnitskaya 48, 119017 Moscow, Russian Federation
Russian Research Centre 'Kurchatov Institute',
pl. Kurchatova 1, 123182 Moscow, Russian Federation
Tel. (7-495) 951 79 93
E-mail: fxela11@yahoo.com, epolyach@gmail.com
N R Nasyrkanov Moscow Institute of Physics and Technology (State University), Institutskii per. 9, 141707 Dolgoprudnyi, Moscow region, Russian Federation

Received 19 June 2009, revised 12 October 2009
Uspekhi Fizicheskikh Nauk **180** (3) 303 – 312 (2010)
DOI: 10.3367/UFNr.0180.201003f.0303
Translated by S D Danilov; edited by A Radzig

Seismic waves are emitted from an earthquake focus (whose size defines the earthquake energy; for definiteness let us assume it be several kilometers). They are low-frequency waves in the infrasonic range, propagating in the solid, elastic Earth. They can further be subdivided into surface and body waves. The former propagate along Earth's surface; the latter, in turn, are classified as longitudinal (elastic compression) waves and transverse (elastic shear) waves. The body waves 'sound', in the literal sense, our planet, and like an X-ray show Earth's interior structure without directly probing its depths (Fig. 1). The speed of longitudinal waves, also referred to as P-waves (primary waves), exceeds that of transverse waves by a factor of 1.7, so that they are first detected by seismographs. The transverse waves are called S-waves (secondary waves).

The propagation speeds of elastic body waves are linked to elastic moduli (the bulk modulus k, and shear modulus μ) and the density ρ of the medium through the well-known expressions

$$v_{\mathrm{P}} = \sqrt{\frac{1}{\rho}\left(k + \frac{4}{3}\,\mu\right)}\,, \qquad v_{\mathrm{S}} = \sqrt{\frac{\mu}{\rho}}\,. \tag{1}$$

According to the available seismic data, Earth can roughly be considered as composed of three main regions: the crust, mantle and core (Fig. 2). The crust is separated from the mantle by a sharp seismic boundary across which the properties of the medium abruptly change (both the propaga-

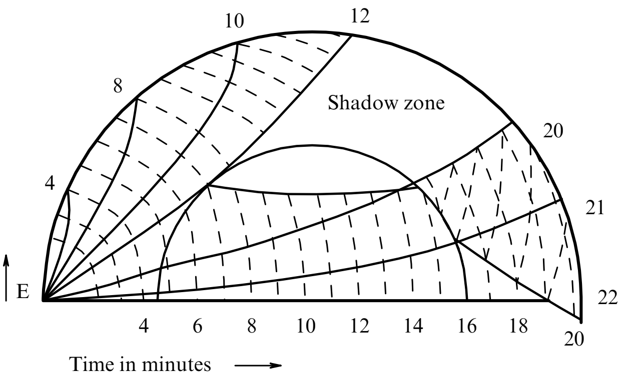

Figure 1. Propagation of seismic P-waves through Earth. Earth's cross section shows trajectories of seismic P-waves emitted from an earthquake focus located directly below the epicenter (point E). The dashed curves (isochrones) specify the propagation time in minutes to various points of Earth's surface. The P-waves are not detected in a broad shadow zone, which is explained by their refraction on the mantle–core interface [2].

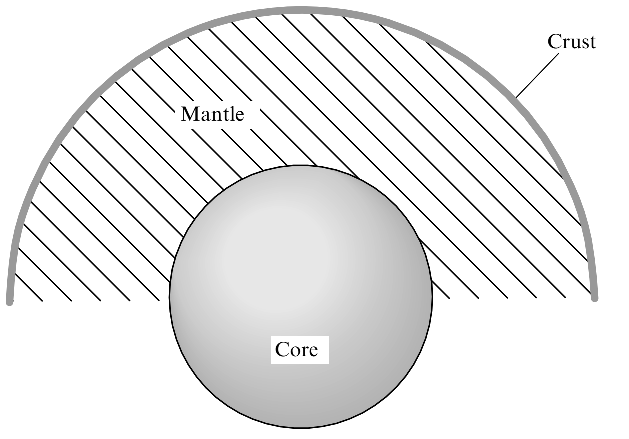

Figure 2. Interior structure of Earth, which consists of three main regions — the crust, mantle, and core.

tion speeds v_P and v_S and density ρ increase). The thickness of Earth's crust is variable, changing from approximately 10 km (with account for the water layer thickness) in the ocean up to 100 km and more in mountain regions of continents. The contribution of Earth's crust to the full mass of Earth and its moment of inertia are small; hence, when considering Earth as a whole, its crust is commonly conceived as a homogeneous layer with an effective thickness of approximately 35 km. Below the crust, at a depth of 35–2885 km, one finds a silicate shell, or Earth's mantle.

Finally, the central part of Earth is located at a depth of 2885–6371 km and comprises the core. Since the average density of Earth is $\rho_{\text{av}} \approx 5.5$ g cm^{-3}, while the densities of granite and basalt composing the surface layer of the crust are, respectively, 2.8 and 3.0 g cm^{-3}, the core must be fairly heavy. Notice that the density of iron meteorites amounts approximately to 7.85 g cm^{-3}.

The speed of P-waves at the mantle–core boundary jumps down from 13.6 to 8.1 km s^{-1}, the speed of S-waves drops from 7.3 km s^{-1} to zero, and the density grows from 5.5 to 10 g cm^{-3}. Since $v_S = 0$ in the core, then, according to Eqn (1), $\mu = 0$, and the core proves to be liquid.

Charles Richter introduced to seismology the notion of the magnitude M_S of an earthquake, which presents a quantitative characteristics of the earthquake linked to the

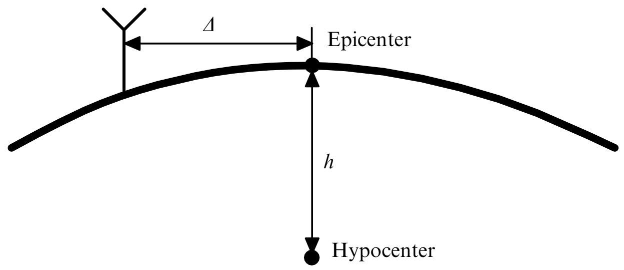

Figure 3. Hypocenter of an earthquake located at depth h, its projection on Earth's surface, called the epicenter, and its distance $\varDelta$ to a seismic station.

parameters of surface waves excited by it (the Richter scale):

$$M_S = \lg \frac{a\,[\mu\text{m}]}{T\,[\text{s}]} + f(\varDelta, h) + C\,, \tag{2}$$

where a is the amplitude of surface excursion in microns in surface waves with the period T expressed in seconds ($T \approx 20$ s), $\varDelta$ is the epicentral distance, h is the distance to the hypocenter (Fig. 3), $f(\varDelta, h)$ is the empirical function reducing all the observations to the standard epicentral distance $\varDelta = 100$ km, and C is the correction taking into account deviations of the ground properties from the standard ones.

The logarithmic scale maps through the single formula a very broad interval of earthquake energy. The strongest earthquakes are characterized by magnitudes exceeding eight on the Richter scale. For example, the catastrophic Chilean earthquake of 22 May 1960 had a magnitude of $M_S = 8.3$. This earthquake is remembered also because after it the entire spectrum of Earth's natural oscillations was recorded. The weakest detectable amplitudes reach negative values (down to -3).

Deep earthquakes emit body waves. The magnitude m characterizing them is defined through a formula analogous to Eqn (2), but with a period $T = 1$ s. Both magnitudes are linked (the Gutenberg–Richter scale):

$$m = 2.5 + 0.63\,M_S\,. \tag{3}$$

The definition of magnitude was selected in such a way that this quantity reflects the energetic properties of earthquakes. Imagine that seismic emission from an earthquake focus consists only of a monochromatic wave with a period $T = 20$ s. The energy of this radiation is then $E_S \sim v^2$, where $v \sim a/T$ is the velocity of vertical ground oscillations in the surface wave. According to Eqns (2) and (3), we find

$$\lg E_S \sim 2 \lg v \sim 2 \lg \frac{a}{T} \approx B M_S + A\,, \tag{4}$$

where

$$B = 2\,, \qquad A = -\lg f(\varDelta, h) - C\,. \tag{5}$$

Because of the more complex radiation spectrum and taking into account some additional factors, one has in practice the following values

$$B \approx 1.5\,, \qquad A \approx 11.8\,. \tag{6}$$

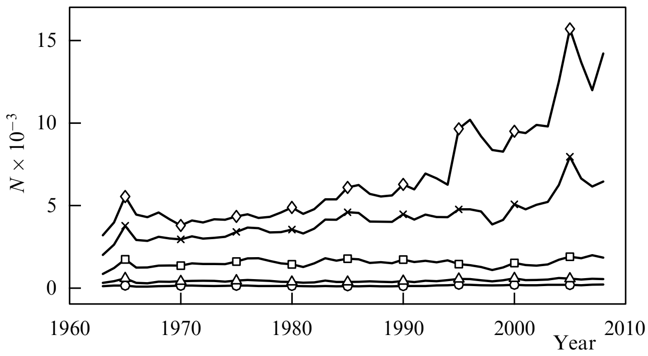

Figure 4. Variations of Earth's global seismic activity (1964–2008). Different symbols are used to label the time evolution curves of annual earthquake number $N(t)$ with a particular magnitude m; the curve labelled with $\diamond$ corresponds to $m \geqslant 4$, $\times$ to $m \geqslant 4.5$, $\square$ to $m \geqslant 5.0$, $\triangle$ to $m \geqslant 5.5$, and $\circ$ to $m \geqslant 6.0$.

Finally, one can write out

$$\lg E_{\mathrm{S}} \approx 11.8 + 1.5\, M_{\mathrm{S}} \,. \tag{7}$$

Hence, an estimate easily follows of the energy of the Chilean earthquake (in erg). Indeed, substituting the magnitude $M_{\mathrm{S}} = 8.3$ into formula (7), one obtains $E_{\mathrm{S}} \sim 10^{24}$ erg.

Earthquakes are subdivided, based on the depth of their hypocenters, into shallow (lithospheric), $h < 70$ km, intermediate (asthenospheric), $h \sim 70-300$ km, and deep, $h > 300$ km. No earthquakes have been recorded at a depth in excess of 720 km.

2. Two components of Earth's seismic activity

Figure 4 displays the time history of the annual number of earthquakes with $m > 4.0$, 4.5, 5.0, 5.5, and 6.0 from 1964 to 2008. Here and below we use catalog data of the National Earthquake Information Center of the U.S. Geological Survey [3], but beginning only from 1964.

As is apparent from Fig. 4, the number of earthquakes with small amplitude, $m \leqslant 4.5$, is growing anomalously, while the number of strong earthquakes, $m > 5$, is staying at approximately the same level. One can suppose that the increase in the number of small earthquakes is a consequence of the increase in the number of operative seismic stations, their sensitivity, and coverage zone, i.e., this increase is similar to the selection effect in astronomy — the prevalence of brightest objects in catalogs.

All curves demonstrate a peak in seismic activity in 1965 and some reduction of activity in 1998. Such a local change in time in the seismic activity and the existence of a quieter interval can be considered as an intrinsic feature of Earth's seismic regime over the period considered. For one thing, the same details are observed not only for different magnitudes, but also in the each hemisphere: the northern, southern, western, and eastern. Indeed, we see common local maxima and minima in seismic activity during the same years once again in Figs 5a, c which present the variability in the number of earthquakes with $m > 4.0$ and 4.5 over the period 1964–2008 in the northern and southern hemispheres. As concerns the interval of so-called quiet seismic activity in 1966–1988, one may notice a mirror symmetry between the earthquake number curves for the northern and southern hemispheres. This antisymmetry is exemplified through negative values of the correlation coefficient computed for the quiet period.

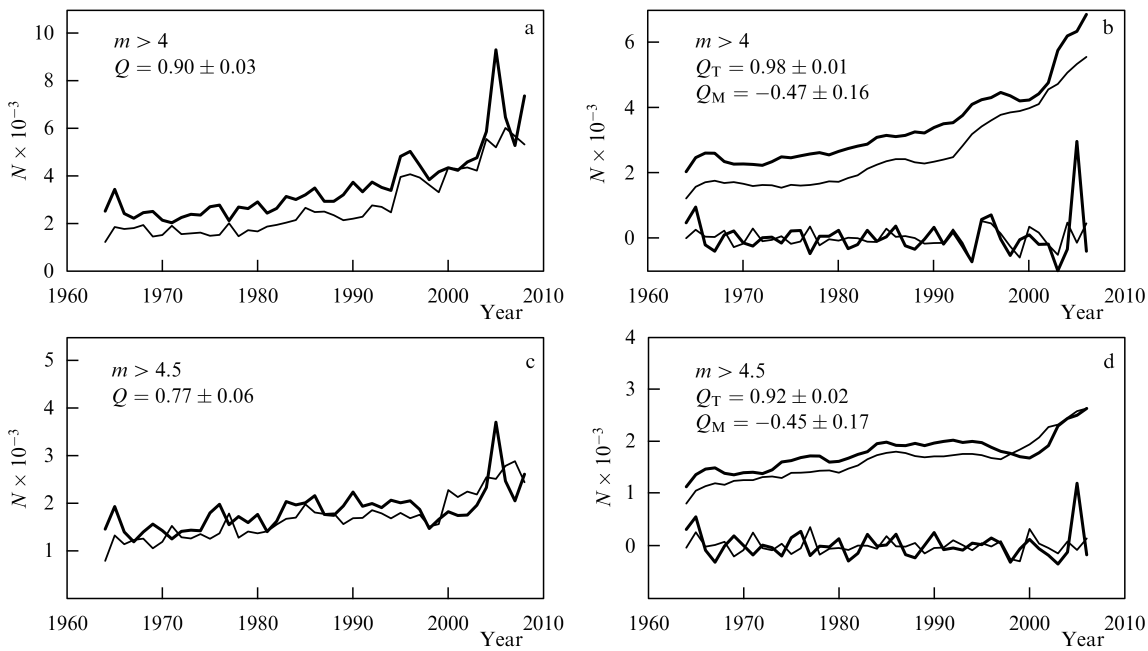

Figure 5. The change in the number of earthquakes with $m \geqslant 4.0$ (a, b) and $m \geqslant 4.5$ (c, d) in the northern (thick lines) and southern (thin lines) hemispheres of Earth. Figure a presents annual data, the coefficient of correlation between the two curves $Q = 0.90 \pm 0.03$; figure b shows running average over five years, the correlation coefficient $Q_{\mathrm{T}} = 0.98 \pm 0.01$, and the difference between annual and averaged curves for each hemisphere, the correlation coefficient $Q_{\mathrm{M}} = -0.47 \pm 0.16$ for the 'quiet' period of 1966–1988 and $Q_{\mathrm{M}} = 0.15 \pm 0.15$ for the whole time interval; figure c — same as in a, the correlation coefficient $Q = 0.77 \pm 0.06$; figure d — same as in b, $Q_{\mathrm{T}} = 0.92 \pm 0.02$ for the two upper curves, $Q_{\mathrm{M}} = -0.45 \pm 0.17$ and $Q_{\mathrm{M}} = 0.00 \pm 0.15$ for the two lower curves for, respectively, the 'quiet' period of 1966–1988 and the whole interval of 1964–2008.

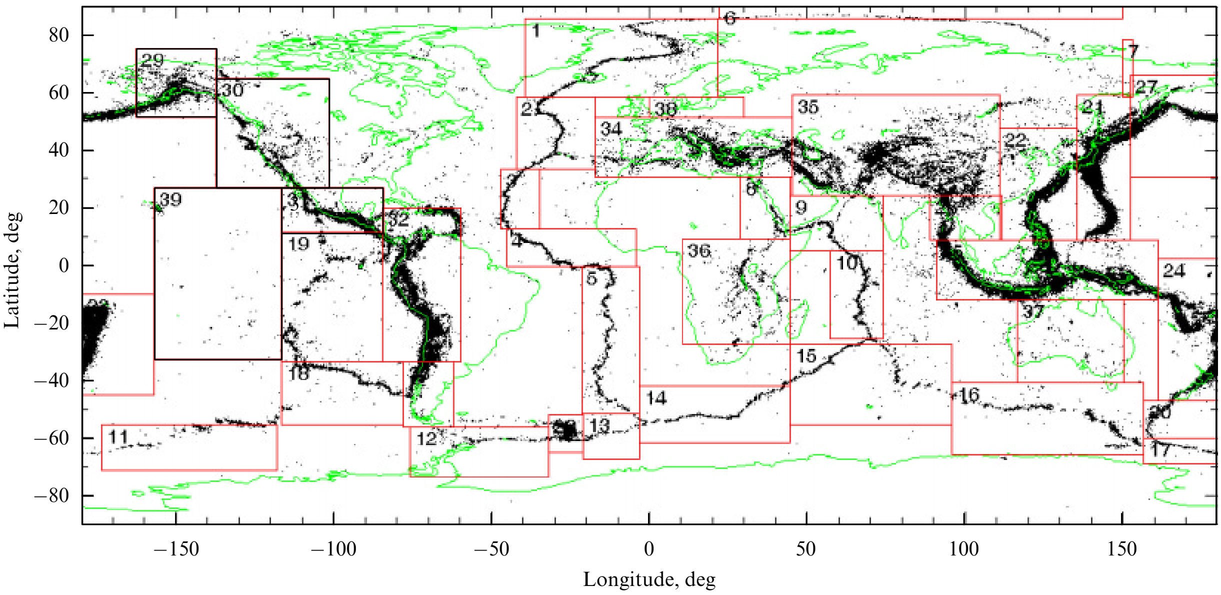

Figure 6. A map of earthquakes with the magnitude $m \geqslant 4.0$ (displayed by dots) for the period of 1964–2008. Also shown are the boundaries and numbers of regions considered in the paper. Regions 1–20 correspond to the zones of spreading, centered around mid-oceanic ridges where volcanic activity contributes to the formation of the ocean crust and causes a gradual shift of tectonic plates in the direction from the ridges. Regions 21–39 correspond to the zones of subduction, i.e., regions of the tectonic plate boundary junction, where one of the plates bends and submerges under the other.

Let us determine the constituents of seismic activity in different hemispheres. Figures 5b, d show smoothed data related to each hemisphere (the running average over five years) and the difference between the annual and smoothed data for selections of earthquakes with magnitudes $m \geqslant 4.0$ and $m \geqslant 4.5$, respectively. While the correlation coefficient for the curves presented in Fig. 5a is $Q = 0.90 \pm 0.03$, that for smoothed curves (Fig. 5b) reaches $Q_{\mathrm{T}} = 0.98 \pm 0.01$ (formulas used to compute the correlation coefficient are given in the Appendix). In the latter case we introduced the subscript T (for total) as an indication that the smoothed curves reflect the variability in the seismic activity of the *entire* globe. Since the correlation $Q < Q_{\mathrm{T}}$ for the curves in Fig. 5a, Q, consequently, contains some small-scale component in addition to the large-scale component Q_{T}. As follows from the shape of the lower curves (Fig. 5b), the small-scale component exhibits a clear mirror symmetry with negative correlation coefficients ($Q_{\mathrm{M}} = -0.47 \pm 0.16$) over the quiet period, whereas no negative correlation between the hemispheres is observed over the entire time interval[1] ($Q_{\mathrm{M}} = 0.15 \pm 0.15$). The notation for the correlation coefficient characterizing the mirror symmetry contains the subscript M. For the smoothed curves (Fig. 5d), the correlation coefficient $Q_{\mathrm{T}} = 0.92 \pm 0.02$; for the small-scale M-component, one finds $Q_{\mathrm{M}} = -0.45 \pm 0.17$ over the quiet period.

Similar results were obtained for the western and eastern hemispheres [4], as well as for the southern and northern parts of the eastern and western hemispheres.

The above analysis demonstrates the existence of two components in Earth's seismic activity (M- and T-components) for the largest regions (their minimum size makes up 1/4 of Earth's surface). Reference [4] presents similar results for regions measuring 1/16 of Earth's surface, and argues that the mirror symmetry of the M-component is observed only during seismically quiet years, while over the remaining years (of high seismic activity) the correlation between M-components can be positive.

[1] In this paper we assume that significant correlations occur for $|Q| \gtrsim 0.5$.

3. M- and T-components in the most seismically active region of Earth

Here we shall try, using several particular and, in our opinion, glowing examples, to illustrate the character of the M-component of seismic activity — thus far only at a phenomenological level. Where can the characteristics of the M-component be exhibited best if not in the most seismically active region of the Earth, with the Eurasian, Pacific, and Indo-Australian Plates meeting each other? The world map in Fig. 6 displays all earthquakes with the magnitude $m \geqslant 4.0$ over the time period 1964–2008. The very broad seismically active regions at the periphery of the Pacific Ocean lie in zones of subduction at plate boundaries; narrower trails of seismic activity follow the mid-oceanic ridges — the zones of spreading (the subduction zones differ also by the considerably deeper depths of the earthquakes).

We have given above a set of examples related to manifestations of mirror symmetry in the M-component of seismicity. In particular, the correlation coefficient between the northern and southern parts of the eastern hemisphere is $Q_{\mathrm{M}} = -0.59 \pm 0.14$ (on averaging over five years of events with $m \geqslant 4.0$ for 1966–1988). By splitting major seismic zones into separate regions and varying their boundaries one can find that the negative correlation coefficient turns out to be the highest between the two regions of Himalayas–Fiji and Philippines–Kamchatka (see Figs 6 and 7). Figure 7 displays averaged positions of earthquake focuses with respect to the fault plane in the depth range 70–120 km for all impacts in the depth interval 120–400 km and also deeper than 400 km. The directions of plate motion can be determined by the relative positions of shallow and deeper earthquakes.

In these branches, where about half of the world's earthquakes occur, $Q_{\mathrm{M}} = -0.74 \pm 0.09$ (on averaging events

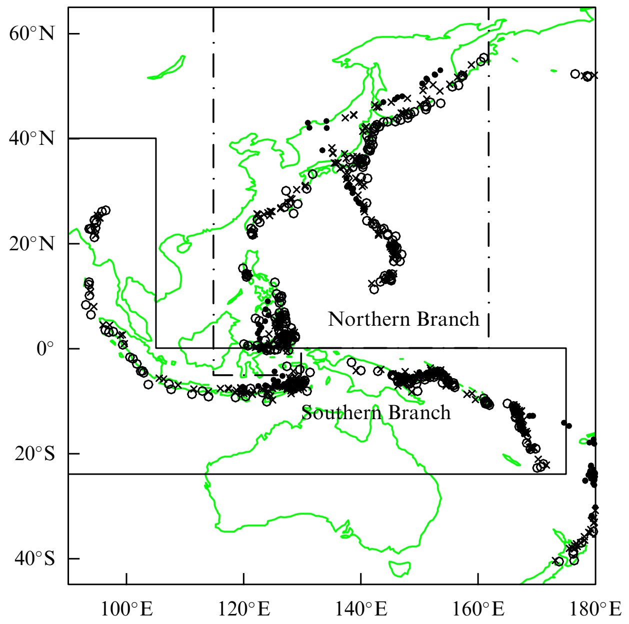

Figure 7. Earth's most active seismic region at the junction of the Eurasian, Pacific, and Indo–Australian plates. Plotted are the earthquakes with hypocenters at 70–120 km (○), 120–400 km (×), and deeper than 400 km (●).

with $m \geqslant 4.0$ over five years). We shall refer to the region located in the northern hemisphere [equatorward from 65° N (northern latitude)] between 115° and 162° E (eastern longitude) as the Northern Branch of the subduction zone. It also includes a zone of the southern hemisphere lying in the belt $0-5°$ S (southern latitude) within the sector $115°-130°$ E (the southern tip of the Philippines zone). The region which begins in the northern hemisphere, in the Himalayas, at 30° N and continues southward to the equator will be referred to as the Southern Branch of the subduction zone. Further, excluding the aforementioned southern Philippines region, this branch includes all earthquakes from the equator to 22° S. The region to the east of the Southern Branch, lying nearly perpendicularly to its main part, will be called the New-Zealand zone. Figure 8a presents the number of earthquakes with $m \geqslant 4.0$ in the Southern and Northern Branches of the subduction zones. Two particular features are apparent — the major growth of activity in both branches (brought about, by all probability, by the growth in the network of seismic stations) and the mirror-symmetric behavior of local extrema in both curves in 1966–1988.

The upper curves in Fig. 8b are essentially those of Fig. 8a but for a running average over five years. The lower curves are obtained by subtracting these averaged curves from the nonaveraged dependences in Fig. 8a. The number and magnitude of seismic events are the same as in Fig. 8a. The mirror symmetry between the lower curves is apparent over the entire time interval. The correlation coefficient between the M-components is $Q_{\rm M} = -0.71 \pm 0.10$ for 1966–1988.

To phenomenologically explore this phenomenon, we shall try to understand the major source of difference between the Northern and Southern Branches. Is this seismic mirror symmetry caused by their mutually perpendicular orientation or the major factor is that the Southern Branch comprises the contact zone between the Indo-Australian and other plates (Pacific and Eurasian), whereas the Northern Branch is just the contact zone between the last two plates?

Figure 7 makes explicit the direction of motion of subducting Pacific and Indo-Australian plates — from shallow earthquakes to deeper ones. As an example, let us consider the region of Honshu Island where the maximum number of earthquakes is observed in the subduction region (the Pacific plate slides under the Eurasian one; see Fig. 9). It is seen that the subduction zone of the Pacific plate, which is practically perpendicular to the direction of its motion, includes the regions Kamchatka Peninsula–Japan–Nampo Islands, the Mariana Islands, the zone of the Philippines, and the region of New Zealand. The subduction zone of the Indo-Australian plate passes through the islands of Sumatra, Java, New Guinea, the Solomons, and the New Hebrides. Let us consider the New Zealand region which geographically belongs to the continuation of the Southern Branch, but is oriented practically transverse to the main part of the Southern Branch, in the same fashion as the Northern Branch. Accordingly, the New Zealand zone, together with the Northern Branch, belongs to the subduction zone of the Pacific plate, while the Southern Branch belongs to the subduction zone of the Indo-Australian plate. Adding New Zealand earthquakes (which increases the total number of events with $m \geqslant 4.0$ by 45%) to the earthquakes of the Southern Branch reduces the absolute value of the negative correlation from $Q_{\rm M} = -0.71 \pm 0.10$ to $Q_{\rm M} = -0.59 \pm 0.14$. Adding these events to the Northern Branch leaves the correlation coefficient $Q_{\rm M} = -0.71 \pm 0.10$ practically unaffected (the correlation for the M-component was computed over the quiet period of 1966–1988). Hence, the dynamics of

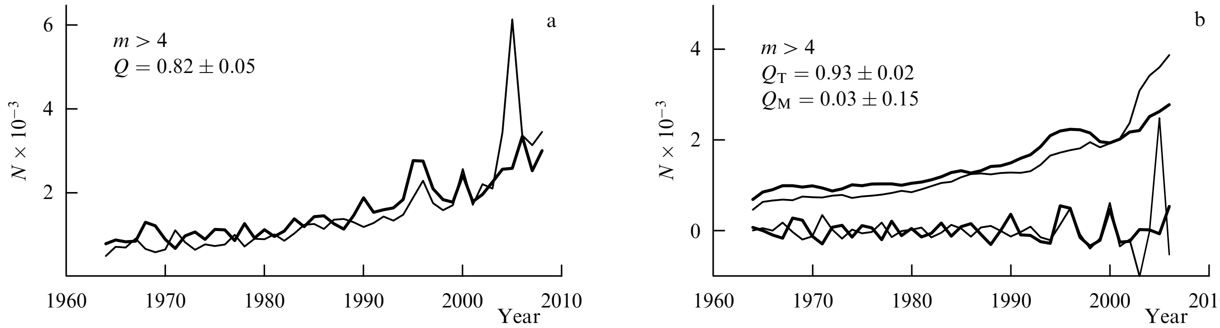

Figure 8. Annual number of earthquakes for 1964–2008 in the Northern (thick line) and Southern (thin line) Branches of the subduction zones. The magnitude of earthquakes is $m \geqslant 4.0$. (a) Annual data, $Q = 0.81 \pm 0.05$. (b) Two components of seismic activity of the Northern and Southern Branches: the T-components averaged over five years (upper curves) and rapidly varying M-components (lower curves). Correlation coefficients for the entire time interval are $Q_{\rm T} = 0.93 \pm 0.02$ and $Q_{\rm M} = 0.03 \pm 0.15$; for the 'quiet' period of 1966–1988, $Q_{\rm M} = -0.71 \pm 0.10$.

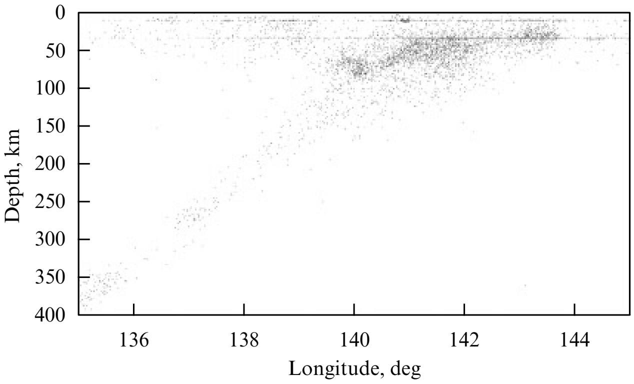

Figure 9. Connection between the depth of earthquakes with $m \geqslant 4.0$ and the longitude in the sector $135° - 145°$ E within the belt $35° - 40°$ N (Honshu Island). One sees a horizontal layer of earthquakes in the body of the Eurasian lithospheric plate (from 0 to 70 km) and an inclined layer of earthquakes along the subducting Pacific plate.

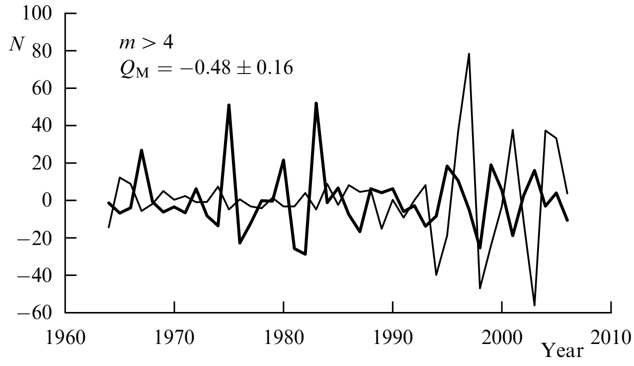

Figure 10. Negative correlation of seismic activity at the junction of three systems of mid-oceanic ridges in the Indian Ocean (its coordinates are 25° S and 70° E), with $Q_M = -0.48 \pm 0.16$. The correlation coefficients were computed over the 'quiet' period of 1966–1988.

earthquakes in the New Zealand region are close to the dynamics of seismicity in the Northern Branch.

4. The M-component of mid-oceanic ridges

The Pacific and Indo-Australian subduction zones form a T-shaped crossing with a center in the vicinity of the equator. If a factor redistributing stresses at the point of a T-shaped junction of tectonic plates is operating in this region, then, seemingly, an analogous factor is also operating at other similar points of fault intersections.

In the Indian Ocean, at a point with coordinates 25° S and 70° E, three mid-oceanic ridges (at the boundary between zones 10 and 15 in Fig. 6) converge to meet each other: the Arabian-Indian Ridge approaches from the north (we take this fault from the Gulf of Aden, at 50° E, to the crossing in the south, at 25° S). From the south–east and south–west the chains of Antarctic Ridges approach the crossing. Analysis shows that the seismicity of the Arabian-Indian Ridge correlates (Q is high by absolute value and negative) with the seismicity of the aforementioned Antarctic Ridges (the thick line in Fig. 10 presents the M-component along the Arabian-Indian Ridge, and the thin one, the M-component along the chain of Antarctic Ridges; the correlation coefficient is $Q = -0.48 \pm 0.16$).

5. Analysis of seismicity of the Alps–Himalayas belt

We shall distinguish between four characteristic zones of seismicity in the Alps-Himalayas belt: the *Himalayan* — from 76° to 95° E and from 26° to 33° N; *Tibetan*, which is an extension of the Himalayan zone to 50° N and includes the Himalayas, Tibet, and Tian Shan; *Sichuan* — from 95° to 106° E and from 20° to 35° N, and *Indochinese*, which is an extension of the Sichuan zone to 15° S. The first two zones are characterized by the latitudinal directions of ridges (folding), i.e., the compression takes place in the meridional direction. Meridional ridges and faults are typical for the third and fourth zones, i.e., the compression proceeds in the west-to-east direction. As we have already seen, an M-component of the seismic process emerges for a perpendicular action of force. From the four zones defined above, one can compose four pair combinations with the transverse action of forces.

Table 1. Correlation coefficients between the averaged (over three years) activity curves (Q_T) and between their deviations (Q_M) from the annual earthquake number for $m \geqslant 4$.

Zone	Q_T	Q_M	Q_M for the quiet period of 1966–1988
Himalayan–Sichuan	0.61 ± 0.10	0.42 ± 0.13	-0.54 ± 0.15
Tibetan–Sichuan	0.59 ± 0.10	0.41 ± 0.13	-0.45 ± 0.17
Tibetan–Indochinese	0.65 ± 0.09	-0.08 ± 0.15	-0.65 ± 0.12
Hymalayan–Indochinese	0.57 ± 0.10	-0.04 ± 0.15	-0.81 ± 0.07

Coefficients of correlation between averaged (over three years) activity curves (Q_T) and between their deviations from annual earthquake number (Q_M) are collected in Table 1 for each of these pairs under the restriction that $m \geqslant 4$.

6. Earth's seismic activity as a function of latitude and its dependence on the depth of epicenters

The dependence of earthquake density on the latitude was addressed previously [5]. The same catalog of the U.S. Geological Survey National Earthquake Information Center VX DAT [3] for 1962–2008 was employed as the database. The graphs of the density of earthquakes versus the latitude of their epicenters, $\rho_\Theta = N_\Theta / S_\Theta$, were constructed. Here, N_Θ is the number of earthquakes in the latitude belt ($\Theta + 5°$; $\Theta - 5°$), and S_Θ is the respective area expressed in units of $2\pi R^2$, where R is Earth's radius. The quantity Θ_n, which stays in correspondence with a certain number of earthquakes N_{Θ_n}, satisfies the condition $\Theta_n = 10n$, where $n = 0, \pm 1, \pm 2, \ldots, \pm 7$. As a consequence, all extrema in curves $N(\Theta)$ or in curves $\rho(\Theta)$ used by us are found only at points $\Theta = \Theta_n$.

Figure 11a presents plots of the distribution of total density of earthquakes as a function of the latitude of epicenters. The five curves correspond to earthquakes with magnitudes $M_b \geqslant 4.0$, 4.5, 5.0, 5.5, and 6.0. One sees a clear dependence of the earthquake density on latitude for all magnitudes and two maxima — the first at 40° N and the

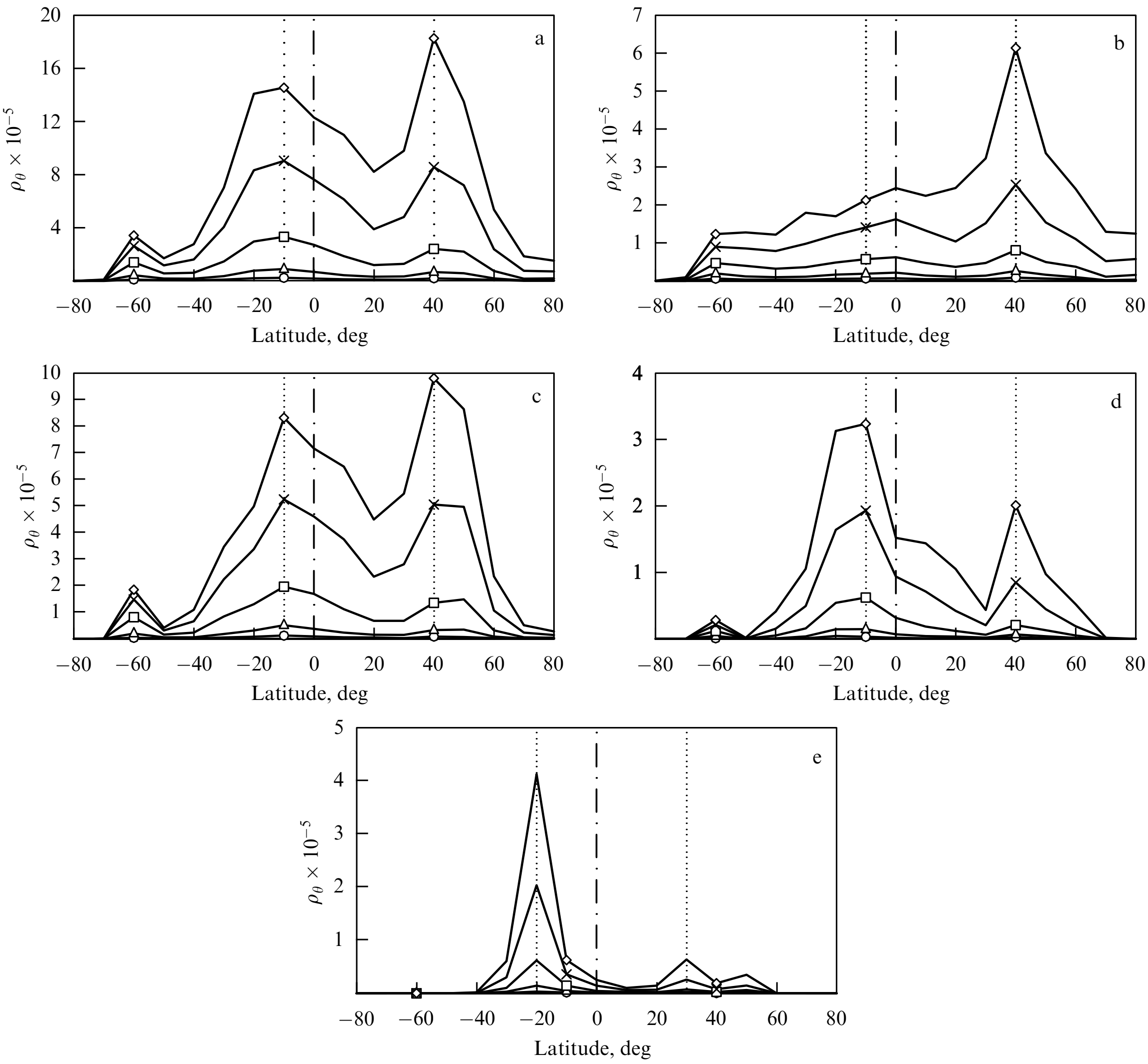

Figure 11. Distribution of earthquake density over latitude for all depths (a), for hypocenters lying at (b) $d < 30$ km, (c) $30 < d < 100$ km, (d) $100 < d < 300$ km, and (e) $d > 300$ km. The curves correspond to magnitudes $m \geqslant 4$ ($\diamond$), $m \geqslant 4.5$ ($\times$), $m \geqslant 5.0$ ($\square$), $m \geqslant 5.5$ ($\triangle$), and $m \geqslant 6.0$ ($\circ$). (Data gathered in 1964–2008.)

second, smaller in amplitude, at 10° S. Apparently, the positions of maxima coincide for all magnitudes. Figure 11b presents similar plots, but for the surface earthquakes whose hypocenters lie at a depth of less than 30 km. It is seen that the number of surface earthquakes detected in the southern hemisphere is essentially smaller than in the northern hemisphere. Plots showing the distribution of earthquakes with hypocenters lying between 30–100 km (Fig. 11c) practically repeat those in Fig. 11a, with the difference being that maximum density amounts to 10^6 instead of 1.8×10^6.

Over the depth range 100–300 km (Fig. 11d), the maximum density of earthquakes is already found in the southern hemisphere. With a further growth in depth, the number of earthquakes occurring in the northern hemisphere drops abruptly, in contrast to that in the southern hemisphere, where earthquakes take place at depths down to 600–700 km (Fig. 11e).

7. On the link between seismic activity and Earth's diurnal rotation

The energy of Earth's diurnal rotation is so large that its variability caused by the Moon, seasonal mass transfer in the atmosphere, and other processes exceeds by many orders of magnitude the total energy of earthquakes. Indeed, simple estimates show that the energy of Earth's diurnal rotation about its axis is given by

$$E = \frac{1}{2}\, I\Omega^2 \sim \frac{1}{5}\, MR^2\Omega^2 = \frac{4\pi}{15}\, R^5\rho\Omega^2 \sim 10^{36}\ \text{erg}\,,$$

where R and ρ are the mean radius and density of Earth, respectively. The energy stored in the surface layer of thickness L [km] is then expressed as

$$E_L \approx E\, 5\, \frac{L}{R} \sim \frac{L}{600} \times 10^{36}\ [\text{erg}]\,,$$

whereas the variation δE_L in the rotation energy of a thin surface layer with depth L, caused by variations in the rotation frequency, is $\delta E_L \sim E_L(2\delta\Omega/\Omega)$.

Figure 12 shows a typical dependence of variation in Earth's rotation frequency on different time scales from 1962 to 2008 according to the data of Ref. [6]. As follows from this figure, the relative frequency variation $\delta\Omega/\Omega \sim 10^{-8}$ over a period of about 10 days, i.e., the variation in the energy of the surface layer with thickness $L \sim 300$ km over this period, amounts to about 10^{28} erg. The

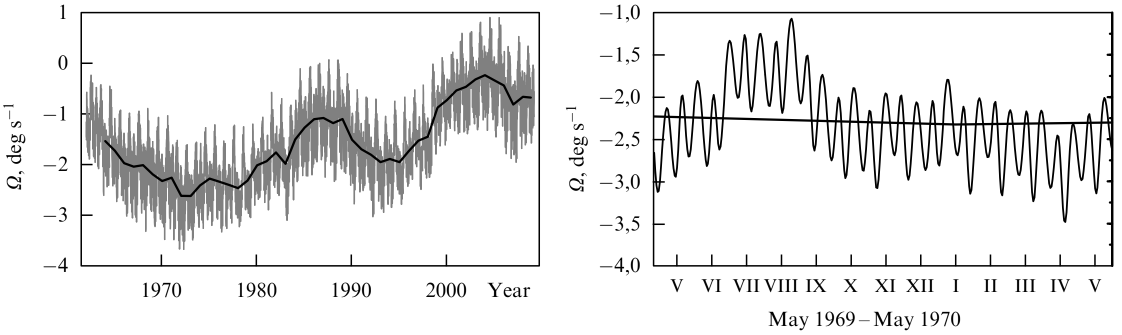

Figure 12. (a) Variability of the rotation frequency $\Omega(t)$ around its mean $\Omega_0 = 72921151.467$ prad s^{-1} and its averaged behavior (black curve; the average taken over the period from 1 July to 30 June of the following year is attributed to the mid-period). (b) Enlargement of the variability curve. Smooth oscillations with a period of 13.6 days, caused by the influence of the Moon, are apparent.

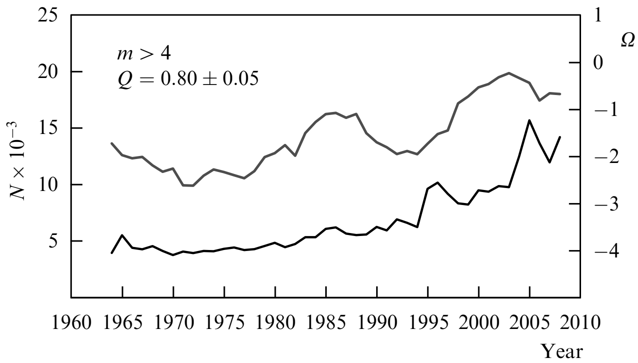

Figure 13. Correlation between the earthquake number $N(t)$ (black curve) and annual mean rotation frequency $\Omega(t)$ (gray curve).

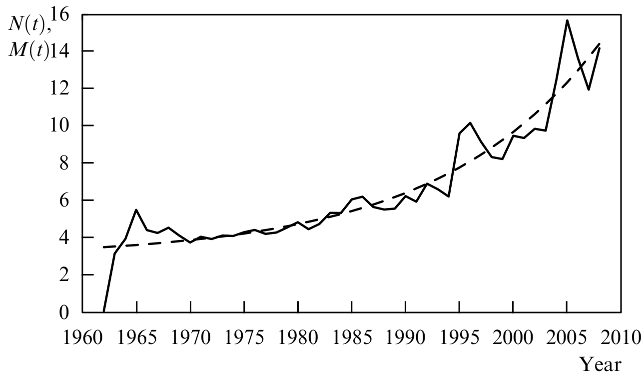

Figure 14. Dependence of earthquake number $N(t)$ (solid curve) and the curve $M(t) = a\exp(bt) + c$ (dashed curve), with the coefficients a, b, and c providing the best fit to $N(t)$.

total annual energy of earthquakes reaches the level of 10^{25} erg. Thus, variations in the rotation energy exceed by several orders of magnitude the mean energy of earthquakes. This fact served as motivation for the hypothesis formulated in Ref. [7] that earthquakes are the consequence of irregularity in Earth's rotation.

This hypothesis was further elaborated in Ref. [8], whose authors try to correlate Earth's seismic activity with the variability of Earth's rotation velocity and the absolute value of its time derivative (characterizing the acceleration or deceleration of Earth's rotation). Let us illustrate their results relying on the data on Earth's rotation from 1962 to 2008. Figure 13 demonstrates a high correlation $Q = 0.80 \pm 0.05$ between the lower curve of the number of earthquakes $N(t)$ with magnitude $m > 4$ and the annual mean frequency $\Omega(t)$ of Earth's rotation.

However, the high correlation coefficient can turn out to be the consequence of selective measurements of earthquakes with small magnitude, mentioned at the beginning of this paper. Indeed, let us look at Fig. 14, which plots the same curve $N(t)$ (solid) together with the dashed curve $M(t) = a\exp(bt) + c$ with coefficients a, b, and c providing the best fit to the curve $N(t)$. Obviously, the exponential growth in the number of relatively weak earthquakes reflects not a growth in Earth's seismic activity, but rather the growth in the number of seismographs and their sensitivity. Indeed, having removed this exponential trend, i.e., dividing $N(t)$ by $M(t)$ (Fig. 15), we are forced to conclude that the correlation between the two curves in question is absent ($Q = -0.13 \pm 0.15$).

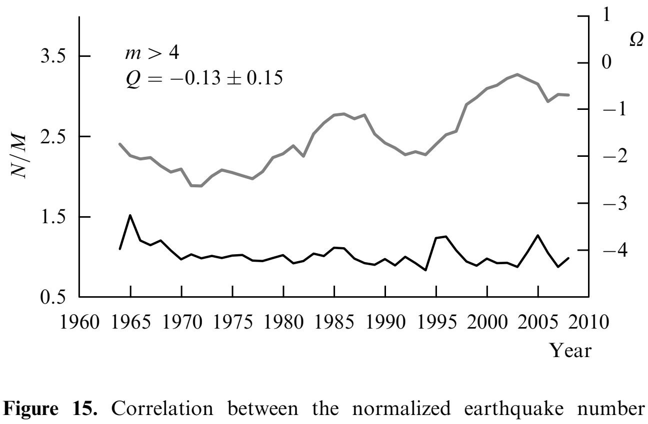

Figure 15. Correlation between the normalized earthquake number $N(t)/M(t)$ (black curve) and annually averaged rotation frequency $\Omega(t)$ (gray curve).

Similar results (with account for the trend) can be found by computing correlations for earthquakes with magnitude $m \geqslant 4.5$. Whereas the correlations for the number of stronger earthquakes are absent from the very beginning.

The analysis of links between the seismic activity and the acceleration of rotation relied on the annual mean dependence of $\Omega(t)$. The correctness of such an analysis can be questioned because averaging removes short-period components contributing, undoubtedly, most strongly to the behavior of $|d\Omega(t)/dt|$ (see Fig. 12).

Thus, the question of the influence of Earth's diurnal rotation on seismic activity remains open. If one assumes the existence of such a connection, then why do not we detect periodic changes in earthquake frequency? The data on earthquakes (especially weak ones) are fully sufficient to carry out a frequency analysis of seismic activity and compare its results with the well-studied spectrum of variability of Earth's rotation frequency. However, the frequency analysis performed by us failed to reveal such a connection.

8. Conclusions

As has already been shown in earlier works [4, 9–13], the seismic activity of Earth can be represented as a combination of two components — the global, slowly varying T-component, and the rapidly varying M-component. This fact has been confirmed on the basis of more complete data covering the period 1964–2008. Also, the principal difference between the behavior of the M-component over the 'quiet' period of 1964–1988 and the rest of the time ('active' periods) was discovered. In the quiet period, the M-component of seismic activity of sufficiently large regions exhibits a negative correlation, whereas the correlation becomes positive in active periods, which is well discernible even by the naked eye, for instance, in the plots of Fig. 5b, d. Since $Q_{\rm M}$ characterizes the correlation between seismic activity curves of neighboring regions (plates), i.e., serves as a numerical characteristic of the M-component, the reason for the opposite signs of contributions to $Q_{\rm M}$ in quiet and active periods could be as follows. When an earthquake happens in one plate, it brings about a reduction in interplate stresses, which then reduces the probability of an earthquake occurring in a neighboring plate. However, in periods of high seismic activity, the interplate stresses are so high that their reduction caused by earthquakes in one region affects the neighboring one only weakly; hence, earthquakes occur in both regions.

It is of interest to relate the quiet period of seismic activity discovered by us with the conduction of underground nuclear tests in the USSR and USA. According to the data of Ref. [14], underground tests were first carried out in the United States in 1957 and 1958, but until 1964 they had a sporadic character. In 1964, both countries launched programs of underground nuclear testing (fully replacing atmospheric tests by 1966) which continued until the end of the 1980s. Figure 16a shows the annual net energy of underground nuclear explosions conducted by the Soviet Union and United States, expressed in units of the Gutenberg–Richter scale (see the Introduction). The most intense tests were conducted precisely over the period from 1966 to 1988. Consequently, one may speculate about a change in the character of Earth's seismic activity over this period.

Characteristic changes in the seismic picture can also be observed for the strongest earthquakes with the magnitude $m \geqslant 8.3$. In Fig. 16b, these earthquakes are shown for the period from 1900 to 2008 and, as follows from the figure, they are absent over the period when underground nuclear tests were carried out (excluding its very beginning).

Thus, there exist at least two classes of dynamical factors governing the variability of seismicity in large tectonic structures:

(a) the global mechanism (T-component) determining the change in time of the total number of strong earthquakes;

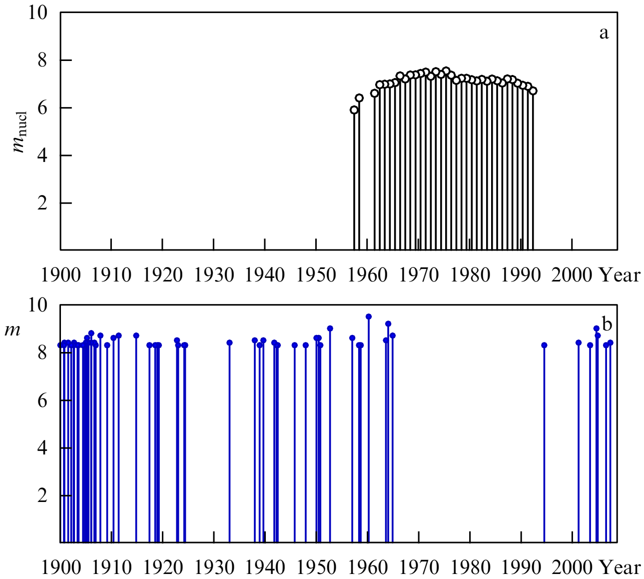

Figure 16. Annual net energy $m_{\rm nucl}$ of underground nuclear explosions carried out by the USSR and USA, expressed on the Gutenberg–Richter scale according to Eqns (3) and (7) for the period 1957–1992 [14]. (b) The strongest earthquakes with the magnitude $m \geqslant 8.3$ from 1900 to 2008 [15]. They were not observed during the period when both countries were conducting their full-sized programs of underground nuclear testing (1966–1988).

(b) the mechanism (M-component) causing variable stresses at junctions of tectonic plates (especially noticeable at crossings) and influencing only weak earthquakes. Arguably, this mechanism is connected to specific oscillations accompanying the displacements of tectonic plates. At present, the oscillatory character of tectonic motions with a period of 2–3 years finds confirmation in data supplied through satellite geodesy [16].

9. Appendix

To compute the correlation coefficient, the following formula for linear correlation (the Pearson correlation) was used:

$$Q = \frac{\sum (x_i - \bar{x})(y_i - \bar{y})}{N\sigma_x \sigma_y} \,,$$

where $\bar{x}$ is the average of quantity x, and $\sigma_x = \sqrt{D_x}$ is its standard deviation:

$$\bar{x} = \frac{1}{N}\sum x_i \,, \qquad D_x = \frac{1}{N}\sum (x_i - \bar{x})^2 \,.$$

Quantities $\bar{y}$ and σ_y are defined accordingly. The error in determining the correlation coefficient is estimated as

$$\Delta Q = \frac{1 - Q^2}{\sqrt{N}} \,.$$

References

1. Richter C F *Elementary Seismology* (San Francisco: W.H. Freeman, 1958) [Translated into Russian (Moscow: IL, 1963)]
2. Zharkov V N *Vnutrennee Stroenie Zemli i Planet* (Interior Structure of the Earth and Planets) (Moscow: Nauka, 1978) [Translated into English (Chur: Harwood Acad. Publ., 1986)]
3. US Geological Survey, National Earthquake Information Center, http://earthquake.usgs.gov

4. Gor'kavyi N N et al. *Fiz. Zemli* (10) 23 (1994)
5. Levin B V, Chirkov E B *Vulkanologiya Seismologiya* (6) 65 (1999)
6. IERS Reference System Service, Earth Rotation Data, http://www.iers.org/products/176/11165/orig/eopc04.62-now
7. Kropotkin P N, Trapeznikov Yu A *Izv. Akad. Nauk SSSR Ser. Geolog.* (11) 32 (1963)
8. Fridman A M, Klimenko A V, in *Nelineinye Volny* (Nonlinear Waves) (Ed. A V Gaponov-Grekhov) (N. Novgorod: IPF RAN, 2003) p. 133
9. Gor'kavyi N N, Minin V A, Taidakova T A, Fridman A M *Astron. Tsirkulyar* (1540) 35 (1989)
10. Gor'kavyi N N et al. *Fiz. Zemli* (10) 33 (1994)
11. Gor'kavyi N N et al. *Fiz. Zemli* (10) 52 (1999) [*Izv., Phys. Solid Earth* **35** 840 (1999)]
12. Gor'kavyi N N, Trapeznikov Yu A, Fridman A M *Dokl. Ross. Akad. Nauk* **338** 525 (1994)
13. Gor'kavyi N N et al. *Fiz. Zemli* (11) 28 (1999) [*Izv., Phys. Solid Earth* **35** 906 (1999)]
14. Database of nuclear tests. Compiled by Wm. Robert Johnston, 2006, http://www.johnstonsarchive.net/nuclear/tests
15. National Geophysical Data Center. The Significant Earthquake Database 1900 – 2008, http://www.ngdc.noaa.gov/hazard/hazards.shtml
16. Tatevyan S K *Issled. Zemli iz Kosmosa* (1) 87 (1999)